



CHORUS

This is the accepted manuscript made available via CHORUS. The article has been published as:

Quantum Limits of Superresolution in a Noisy Environment

Changhun Oh, Sisi Zhou, Yat Wong, and Liang Jiang

Phys. Rev. Lett. **126**, 120502 — Published 26 March 2021

DOI: [10.1103/PhysRevLett.126.120502](https://doi.org/10.1103/PhysRevLett.126.120502)

Quantum limits of superresolution in noisy environment

Changhun Oh,^{1,*} Sisi Zhou,^{2,1} Yat Wong,¹ and Liang Jiang^{1,†}

¹*Pritzker School of Molecular Engineering, The University of Chicago, Chicago, Illinois 60637, USA*

²*Department of Physics, Yale University, New Haven, Connecticut 06511, USA*

(Dated: February 8, 2021)

We analyze the ultimate quantum limit of resolving two identical sources in a noisy environment. We prove that in the presence of noise causing false excitation, such as thermal noise, quantum Fisher information (QFI) of arbitrary quantum states for the separation of the objects, which quantifies the resolution, always converges to zero as the separation goes to zero. It contrasts with a noiseless case where it has been shown to be non-zero for a small distance in various circumstances, revealing the superresolution. In addition, we show that false excitation on an arbitrary measurement, such as dark counts, also makes the classical Fisher information (CFI) of the measurement approach to zero as the separation goes to zero. Finally, a practically relevant situation, resolving two identical thermal sources, is quantitatively investigated by using QFI and CFI of finite spatial mode multiplexing, showing that the amount of noise poses a limit on the resolution in a noisy system.

Rayleigh criterion poses a limit of resolution of two incoherent objects in classical optics [1, 2]. Recently, inspired by quantum optics and quantum metrology, superresolution overcoming the Rayleigh limit has been proposed by replacing a conventional direct imaging technique with structured measurement techniques in a weak source regime [3]. Since the breakthrough, the superresolution technique has been generalized for two incoherent thermal sources [4], arbitrary quantum states of two objects [5], two-dimensional imaging [6], three-dimensional imaging [7, 8], estimating spatial deformation [9], and an arbitrary number of sources [10–13], and it has been also studied from the perspective of channel discrimination [14, 15]. Also, many proof-of-principle experiments have demonstrated that elaborately constructed measurements enable surpassing the Rayleigh limit in practice [16–20]. The main idea of revealing superresolution is to show that the quantum Fisher information (QFI) of two objects' separation, the inverse of which limits the estimation error of the separation, is still non-zero when the separation converges to zero. This behavior contrasts with a conventional direct imaging method whose classical Fisher information (CFI) vanishes as the separation drops to zero, making the estimation error of the separation diverge for a small separation.

More recently, the effects of noise on superresolution techniques start to be analyzed. The CFI of two point sources' separation using a spatial mode demultiplexing scheme has been shown to vanish in the presence of dark counts [21] or measurement crosstalk [22] when the separation is small. However, these analyses are restricted to specific measurement schemes. Meanwhile, the QFI of resolving two incoherent thermal point sources also vanishes for small separations in the presence of thermal background noise [23]. In this case, the influence of detection noise is not systematically analyzed. Besides, previous studies are limited to uncorrelated classical states such as thermal states and weak point sources. More gen-

eral quantum states need to be analyzed for applications on microscopy where we can manipulate quantum states of light emitted from sources to improve resolution.

In this Letter, we consider a more general situation of resolving two identical sources in arbitrary quantum states, assuming a generic noise model inevitable in experiments, which we call excitation noise. Excitation noise is a type of noise causing false excitation that cannot be distinguished from signal photons, which includes thermal background noise and dark counts. We first prove that excitation noise makes QFI to vanish for small separations, which indicates that the resolution of two close sources is inherently vulnerable to noise in practical imaging processes. We also provide a quantitative analysis of noise in resolving two identical incoherent thermal sources. We then show that the CFI of arbitrary measurement affected by excitation noise on detectors vanishes for small separations. Notably, our results reproduce previous studies about the impact of noises on particular imaging processes and states [21–23]. Finally, we show that in the presence of thermal noise, a finite spatial mode demultiplexing (fin-SPADE) measurement is nearly optimal when a signal-to-noise ratio (SNR) is large.

The model.— Consider two identical sources with a separation $s > 0$ that emit light described by two orthogonal creation operators $\hat{c}_{1,2}^\dagger$. The emitted light reaches to the image plane with being attenuated such that $\hat{c}_{1,2}^\dagger \rightarrow \sqrt{\eta}\hat{a}_{1,2}^\dagger - \sqrt{1-\eta}\hat{u}_{1,2}^\dagger$ with environmental modes $\hat{u}_{1,2}^\dagger$ and being distorted as

$$\hat{a}_1^\dagger \equiv \int_{-\infty}^{\infty} dx \psi(x - s/2) \hat{a}_x^\dagger, \quad \hat{a}_2^\dagger \equiv \int_{-\infty}^{\infty} dx \psi(x + s/2) \hat{a}_x^\dagger. \quad (1)$$

Here, $\psi(x)$ represents the point-spread function (PSF) of the imaging system, assumed to be real for simplicity. Also, the mode operators for different positions satisfy the canonical commutation relation (CCR) $[\hat{a}_x, \hat{a}_{x'}^\dagger] =$

$\delta(x-x')$. In general, the two mode operators do not obey the CCR since the two PSFs $\psi(x \pm s/2)$ have a non-zero overlap, i.e., $[\hat{a}_1, \hat{a}_2^\dagger] \neq 0$. Thus, we define symmetric and antisymmetric modes \hat{a}_\pm to orthogonalize them [3–5, 7],

$$\hat{a}_\pm \equiv \frac{\hat{a}_1 \pm \hat{a}_2}{\sqrt{2(1 \pm \delta)}}, \quad \delta(s) \equiv \int_{-\infty}^{\infty} dx \psi(x + s/2) \psi(x - s/2), \quad (2)$$

which satisfy the CCR, i.e., $[\hat{a}_+, \hat{a}_-] = 0$. Now, the overall dynamics can be captured as

$$\hat{c}_\pm^\dagger \equiv \frac{\hat{c}_1^\dagger \pm \hat{c}_2^\dagger}{\sqrt{2}} \rightarrow \sqrt{\eta_\pm} \hat{a}_\pm^\dagger - \sqrt{1 - \eta_\pm} \hat{u}_\pm^\dagger, \quad (3)$$

where $\eta_\pm \equiv (1 \pm \delta)\eta$ represent effective attenuation rates, and \hat{u}_\pm represent auxiliary modes. Furthermore, the imaging process of estimating the separation s can be described by the following dynamics of the mode operators [5, 24],

$$\frac{d\hat{a}_\pm}{ds} = i[\hat{H}_\pm^{\text{eff}}, \hat{a}_\pm], \quad (4)$$

where the effective Hamiltonians are written as

$$\hat{H}_\pm^{\text{eff}} = i \frac{d\theta_\pm}{ds} (\hat{c}_\pm^\dagger \hat{v}_\pm - \hat{c}_\pm \hat{v}_\pm^\dagger) - i B_\pm (\hat{a}_\pm \hat{b}_\pm^\dagger - \hat{a}_\pm^\dagger \hat{b}_\pm), \quad (5)$$

where \hat{v}_\pm are the environmental mode operators before the transformation, $\theta_\pm \equiv \arccos \sqrt{\eta_\pm}$,

$$\hat{b}_\pm \equiv \frac{1}{B_\pm} \frac{\partial \hat{a}_\pm}{\partial s}, \quad \text{and} \quad B_\pm \equiv -\frac{\epsilon_\pm}{2\sqrt{1 \pm \delta}}. \quad (6)$$

Thus, mode operators \hat{b}_\pm represent the derivative of the spatial modes, $\hat{a}_\pm(s + ds) \approx \hat{a}_\pm(s) + \partial_s \hat{a}_\pm(s) ds$. We have also defined the following parameters:

$$\epsilon_\pm^2 \equiv \Delta k^2 \mp \beta - \frac{\gamma^2}{1 \pm \delta}, \quad \gamma \equiv \delta'(s), \quad \Delta k^2 \equiv \beta(0), \quad (7)$$

$$\beta(s) \equiv -\delta''(s) = \int_{-\infty}^{\infty} dx \frac{d\psi(x + s/2)}{dx} \frac{d\psi(x - s/2)}{dx}. \quad (8)$$

Here, γ represents the variation of the overlap from the changes of the separation s , Δk^2 accounts for the variance of the momentum operator $-i\partial_x$, and β represents interference between the derivatives of the PSFs. The effective Hamiltonians show that when the separation s changes, the attenuation to the environment \hat{u}_\pm varies as well as the derivative modes \hat{b}_\pm are excited through the beam-splitter-like Hamiltonian, which is the last term in Eq. (5). Note that the model assumes that the light evolves under a passive transformation before reaching to the image plane and that since we use the Heisenberg picture, the emitted light from sources can be an arbitrary quantum state.

QFI in a noisy system.— From the perspective of quantum metrology, resolution can be quantified by the

QFI of the separation s [3]. QFI $H(\theta)$ of a quantum state $\hat{\rho}(\theta)$ for an unknown parameter θ gives a lower bound of the estimation error for θ , $\Delta^2\theta \geq 1/MH(\theta)$, which is the so-called quantum Cramér-Rao inequality [25–28]. Here, M is the number of independent trials. Note that the quantum Cramér-Rao inequality indicates that estimation error diverges if QFI vanishes.

Before we present our main result, we define excitation noise as a type of noise that transforms any quantum state to be a full-rank state. Physical interpretation of the noise is that it introduces false excitation indistinguishable from the signal. Thermal background noise is such noise, which is described by a beam-splitter interaction with an environmental mode in a thermal state of a non-zero photon number [29], because thermal background noise transforms a state into a full-rank state.

Now, we present our main result:

Proposition 1. For imaging processes in the presence of excitation noise, the QFI for the separation s of two identical sources in arbitrary quantum states converges to zero as $s \rightarrow 0$.

Proof. Let $\hat{\rho}(s)$ be an arbitrary quantum state of light at the image plane, emitted by two identical sources separated by s . First, because two objects are identical, replacing s by $-s$ does not change the description of the system. Thus, we have $d\hat{\rho}/ds \propto s\hat{\sigma}$ with a Hermitian operator $\hat{\sigma}$ for small $s \ll 1$, which is explicitly shown in Ref. [24]. Meanwhile, since noise may occur any relevant modes in the system, the quantum state $\hat{\rho}(s)$ is full-rank after undergoing excitation noise.

Recall that QFI is written as $H(s) = \text{Tr}[\hat{\rho}(s)\hat{L}(s)^2]$, where \hat{L} is symmetric logarithmic derivative (SLD) operator satisfying the equation $\partial_s \hat{\rho}(s) = [\hat{\rho}(s)\hat{L}(s) + \hat{L}(s)\hat{\rho}(s)]/2$ [25–28]. Writing the quantum state in a spectral decomposition form $\hat{\rho}(s) = \sum_i p_i |\psi_i\rangle\langle\psi_i|$ and using $d\hat{\rho}/ds \propto s\hat{\sigma}$, the SLD operator can be written as [28]

$$\begin{aligned} \hat{L}(s) &= 2 \sum_{i,j:p_i+p_j>0} \frac{\langle\psi_i|\partial_s \hat{\rho}(s)|\psi_j\rangle}{p_i + p_j} |\psi_i\rangle\langle\psi_j| \\ &\approx 2s \sum_{i,j:p_i+p_j>0} \frac{\langle\psi_i|\hat{\sigma}|\psi_j\rangle}{p_i + p_j} |\psi_i\rangle\langle\psi_j| + O(s^2). \end{aligned} \quad (9)$$

By the definition of excitation noise, $p_i + p_j > 0$ for all i, j and $p_i + p_j$ does not converge to zero as $s \rightarrow 0$; hence, $H(s) = \text{Tr}[\hat{\rho}\hat{L}^2] \propto s^2 \rightarrow 0$ as $s \rightarrow 0$ [30]. (A similar argument has been used in the context of quantum spectroscopy [31].) \square

Note that although we assumed excitation noise for simplicity, it is sufficient for a final state to be full-rank only in the subspace of signal operator $\hat{\sigma}$ to prove the same result. The proposition can be intuitively explained by noting that the signal in the imaging system approaches zero for $s \rightarrow 0$, indicated by $d\hat{\rho}/ds \propto s\hat{\sigma}$,

while the noise ratio remains finite. Therefore, the SNR vanishes for small s , which leads to vanishing QFI. In contrast, when the quantum state is not full-rank in the support of $\hat{\sigma}$ around $s = 0$, there exists $p_i > 0$ and $|\psi_i\rangle$ such that $p_i \rightarrow 0$ as $s \rightarrow 0$ and a projection measurement onto $|\psi_i\rangle\langle\psi_i|$ gives a non-zero QFI element. Therefore, the QFI may not vanish for small s , which accounts for non-zero QFI for noiseless cases [3–5].

Note that attenuation channels, where a vacuum state occupies the environmental mode \hat{e} , do not introduce false excitation but diminish the signal. Thus, the QFI of s does not necessarily vanish as $s \rightarrow 0$. We emphasize that the proposition does not rule out the possibility of superresolution overcoming the Rayleigh limit but implies that when the objects are close and the system is noisy, the QFI of the separation can be extremely small. We supply an important example to analyze the effect of noise in the following section.

Two identical thermal sources.— Consider two incoherent thermal sources with an unknown separation s . When the modes \hat{a}_1, \hat{a}_2 are occupied by thermal states of the mean photon number N_s , the symmetric and antisymmetric modes \hat{a}_+ and \hat{a}_- can also be described by thermal states of the mean photon number $\eta N_s(1 + \delta)$ and $\eta N_s(1 - \delta)$, respectively [4, 5]. Introducing thermal noise characterized by the same mean photon number N_n onto the relevant modes \hat{a}_\pm and \hat{b}_\pm , the quantum state is written as the product of the states of symmetric and antisymmetric modes, $\hat{\rho} = \hat{\rho}_+ \otimes \hat{\rho}_-$, where

$$\hat{\rho}_\pm(s) = \hat{\rho}_T(\eta N_s(1 \pm \delta(s)) + N_n) \otimes \hat{\rho}_T(N_n). \quad (10)$$

Here, each mode corresponds to \hat{a}_\pm, \hat{b}_\pm , respectively, and $\hat{\rho}_T(N)$ represents a thermal state with the mean photon number N .

Using the QFI formula of Gaussian states [32–38], we obtained the QFI of the separation s [24], $H(s) = H_+(s) + H_-(s)$ with

$$H_\pm(s) = \frac{\eta^2 N_s^2 \gamma^2}{(\eta N_s(1 \pm \delta) + N_n + 1)(\eta N_s(1 \pm \delta) + N_n) - \frac{2\eta^2 N_s^2 [(1 \pm \delta)(\delta''(0) \mp \delta''(s)) + \gamma^2]}{(2N_n + 1)(2\eta N_s(1 \pm \delta) + 2N_n + 1) - 1}}. \quad (11)$$

Here, $H_\pm(s)$ represent the QFI from symmetric and antisymmetric modes, respectively. The first and second term accounts for the changes of the mean photon number on mode \hat{a}_\pm from the change of effective attenuation factors η_\pm and the transformation of the spatial modes' shape $\hat{a}_\pm(s)$ into $\hat{a}_\pm(s + ds) \approx \hat{a}_\pm(s) + ds\partial_s\hat{a}_\pm$, respectively.

The QFI recovers previous results when $N_n = 0$ in Refs. [4, 5]. More importantly, the QFI vanishes as $s \rightarrow 0$ unless $N_n = 0$. Fig. 1 (a) and (b) compare the QFI $H(s)$ in the ideal and noisy cases with the Gaussian PSF, $\psi(x) = e^{-x^2/4\sigma^2}/(2\pi\sigma^2)^{1/4}$. A remarkable difference between the two cases is that as $s \rightarrow 0$, the QFI in

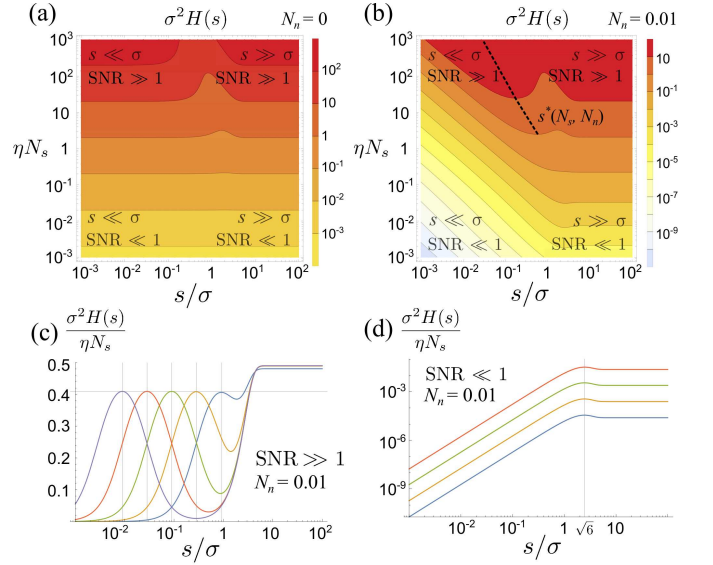


FIG. 1. QFI with respect to s and N_s with (a) $N_n = 0$ (noiseless), (b) $N_n = 0.01$. In the noiseless case, the quantum Fisher information does not decrease as s decreases. However, even with a small amount of noise photons, the QFI drops for small s . The dotted line in (b) shows local maxima of QFI for fixed ηN_s , $N_n > 0$, and $\text{SNR} \gg 1$ as shown in (c). (c) Normalized QFI when $\text{SNR} \gg 1$ with respect to s with $\eta N_s = 10^4, 10^3, 10^2, 10, 1$ from the left to the right and, $N_n = 0.01$. The horizontal line represents $H(s^*)$ and the vertical lines s^* (see the main text). It captures the non-monotonic behavior of QFI. (d) Normalized QFI when $\text{SNR} \ll 1$ with $\eta N_s = 10^{-4}, 10^{-3}, 10^{-2}, 10^{-1}$ from the bottom.

the noisy case rapidly drops whereas it does not change in the ideal case. For example, when the separation s is 0.01σ and the mean signal photons ηN_s is 1, the QFI $H(s)$ is $0.5/\sigma^2$ and $6 \times 10^{-4}/\sigma^2$ for the noiseless case and the noisy case with $N_n = 0.01$, respectively, which clearly shows that even a small amount of noise can be critical to the resolution.

Let us consider the regime where the SNR is large, $\text{SNR} \equiv \eta N_s/N_n \gg 1$. In this regime, Fig. 1 (c) shows another interesting feature of QFI; it is not monotonic with respect to s . For a small separation $s \ll \sigma$ in the regime, the QFI for the Gaussian PSF can be approximated by

$$H(s) \approx \frac{4\eta^2 N_s^2 s^2}{\eta^2 N_s^2 s^4 + 8\eta N_s s^2 \sigma^2 + 64N_n(N_n + 1)\sigma^4}, \quad (12)$$

which has the local maximum

$$H(s^*) \approx \frac{\eta N_s}{2\sigma^2} \frac{\sqrt{N_n^2 + N_n}}{(N_n + \sqrt{N_n^2 + N_n})(\sqrt{N_n^2 + N_n} + N_n + 1)} \underset{N_n \ll 1}{\approx} \frac{\eta N_s}{2\sigma^2} \frac{1}{1 + 2\sqrt{N_n}} \quad (13)$$

at $s^* = 2\sqrt{2}(N_n^2 + N_n)^{1/4}\sigma/\sqrt{\eta N_s}$, as shown in Fig. 1 (c). Here s^* is a characteristic length scale, and if $s \ll s^*$,

the QFI can be further approximated as

$$H(s) \approx \frac{\eta^2 N_s^2}{N_n(N_n + 1)} \Delta k^4 s^2 = \frac{\eta^2 N_s^2}{N_n(N_n + 1)} \frac{s^2}{16\sigma^4} \quad (14)$$

$$\underset{N_n \ll 1}{\approx} \frac{\eta^2 N_s^2}{N_n} \frac{s^2}{16\sigma^4} \quad \text{if } \eta N_s \gg N_n \text{ and } s \ll s^*.$$

One can observe that when $\text{SNR} \gg 1$, $N_n \ll 1$ and $s \ll s^*$, the QFI per a signal photon is proportional to the SNR $H(s)/\eta N_s \propto \eta N_s/N_n$, which is consistent with the previous results [21, 23]. Also, the QFI decreases quadratically as $s \rightarrow 0$.

On the other hand, when the SNR is small, i.e., $\eta N_s/N_n \ll 1$, and the separation is small, $s \ll \sqrt{6}\sigma$, the QFI is approximated by

$$H(s) \approx \frac{\eta^2 N_s^2}{2N_n(N_n + 1)} [3\Delta k^4 + \delta^{(4)}(0)] s^2 \quad (15)$$

$$= \frac{\eta^2 N_s^2}{N_n(N_n + 1)} \frac{3s^2}{16} \quad \text{if } \eta N_s \ll N_n \text{ and } s \ll \sqrt{6}\sigma,$$

which is shown in Fig. 1 (d). Again, when $N_n \ll 1$, the QFI per a signal photon is proportional to the SNR, $H(s)/\eta N_s \propto \eta N_s/N_n$, and decreases quadratically as $s \rightarrow 0$.

Finally, for a large separation $s \gg \sigma$, the QFI can be approximated as $H(s) \approx 2\eta^2 N_s^2 \Delta k^2 / [2N_n^2 + \eta N_s + 2N_n(\eta N_s + 1)]$, which shows that the noise decreases the QFI for a large separation as well.

As a remark, we compare the QFI in Eq. (11) with the one obtained in Ref. [23] where the same type of noise was studied in the imaging process. The discrepancy of the expression is present because the noise model of Ref. [23] assumes that noise occurs only on the modes \hat{a}_\pm whereas our noise model assumes the same amount of noise on \hat{b}_\pm modes. Nevertheless, the previous result has also revealed that the QFI vanishes as $s \rightarrow 0$ because the rank of the quantum state does not change around $s = 0$ in the first order of s even if we assume $N_n = 0$ for \hat{b}_\pm modes.

Noisy detectors.— As pointed out in Ref. [23], analyzing QFI might not be appropriate to consider the effect of dark counts because QFI is a measurement-independent quantity while dark counts are a feature of the measurement device. To analyze the impact of dark counts, we employ CFI $F(\theta)$ for an unknown parameter θ , the inverse of which gives a lower bound of estimation error for a given measurement apparatus, $\Delta^2\theta \geq 1/MF(\theta)$ [39–42]. By introducing the following proposition, we show that excitation noise on detectors makes the CFI vanish.

Proposition 2. Consider a quantum state that satisfies $\partial_\theta \hat{\rho} \approx \theta \hat{\sigma}$ for small θ with a Hermitian operator $\hat{\sigma}$ and a positive-operator-valued-measurement (POVM) $\{\hat{\Pi}_k\}_{k \in K}$ satisfying $\hat{\Pi}_k \geq 0$, $\sum_{k \in K} \hat{\Pi}_k = \mathbb{1}$. Here, K is an index set of measurement outcomes. If the support of the probability distribution $p_k = \text{Tr}[\hat{\rho}(\theta)\hat{\Pi}_k]$,

$\{k \in K | p_k > 0\}$, does not change as $\theta \rightarrow 0$, the CFI converges to zero as $\theta \rightarrow 0$.

Proof. Recall that the CFI of probability distribution $\{p_k\}$ is given by [39–42]

$$F(\theta) = \sum_{p_k > 0} \frac{1}{p_k} \left(\frac{\partial p_k}{\partial \theta} \right)^2. \quad (16)$$

The probability of obtaining outcome k by measuring a quantum state $\hat{\rho}(\theta)$ with POVM $\{\hat{\Pi}_k\}_{k \in K}$ and its derivative with respect to θ are given by

$$p_k = \text{Tr}[\hat{\Pi}_k \hat{\rho}(\theta)] \quad \text{and} \quad \frac{\partial p_k}{\partial \theta} \approx \theta \text{Tr}[\hat{\Pi}_k \hat{\sigma}]. \quad (17)$$

Therefore, the CFI of small θ is written as

$$F(\theta) = \sum_{p_k > 0} \frac{1}{p_k} \left(\frac{\partial p_k}{\partial \theta} \right)^2 \approx \theta^2 \sum_{p_k > 0} \frac{1}{p_k} \left(\text{Tr}[\hat{\Pi}_k \hat{\sigma}] \right)^2. \quad (18)$$

Similar to QFI, CFI converges to zero as $\theta \rightarrow 0$ unless there exists p_k such that $p_k \rightarrow 0$ [30]. \square

The proposition can be understood similarly to Proposition 1. The proposition provides a necessary condition to prevent the CFI of a measurement setting from vanishing for a small separation s . For example, dark counts are a kind of excitation noise on detectors, causing false excitations on all relevant detectors. Dark count rates are generally non-zero in all relevant detectors in practice; thus, the support of the probability distribution does not change, and it is natural to expect that the CFI of separation s vanishes $F(s) \rightarrow 0$ as $s \rightarrow 0$ in experiment. Moreover, the proposition can be applied to measurement crosstalk, which may arise for fin-SPADE scheme [22]. It makes all measurement outcomes mixed so that eventually the probability of obtaining each outcome becomes non-zero. Also, the proposition shows the limitation of direct imaging, homodyne detection, and heterodyne detection [43] which always gives a non-zero probability of each outcome for generic PSFs even in the noiseless case. As a final remark, proposition 2 does not imply the failure of superresolution; it suggests that excitation noise on detectors can pose a limit on the resolution as for QFI in the previous section.

Finite spatial mode demultiplexing.— Finally, we analyze achievable resolution using the fin-SPADE measurement. In the noiseless case, the fin-SPADE scheme employs a photon-counting for each Hermite-Gaussian mode $h_q(x)$ on the image plane, which is optimal if an enough number of Hermite-Gaussian modes are accessible in experiment [3, 5]. In general, the analytical expression of the CFI of the fin-SPADE scheme is difficult to obtain due to the statistical correlations between different modes of the measurement. We thus obtain the lower bound of

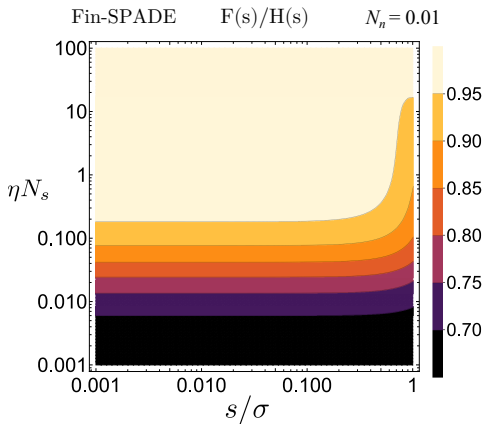


FIG. 2. Relative CFI of fin-SPADE to QFI with respect to different separation s and mean signal photon number ηN_s .

the CFI using an inequality $F(\theta) \geq \dot{\vec{\mu}}^T C^{-1} \dot{\vec{\mu}}$, where $\vec{\mu}$ and C denote the mean and covariance matrix of the outcome distribution, and $\dot{\vec{\mu}} \equiv \partial_s \vec{\mu}$ [44]. We provide more details on the CFI and the numerical method in Ref. [24]. We consider a finite number of Hermite-Gaussian modes h_q with $0 \leq q \leq Q - 1$ with $Q = 15$ in the presence of thermal noise in the problem of resolving two incoherent thermal sources. We confirmed that increasing Q larger than 15 does not change the CFI for $10^{-3} \leq s/\sigma \leq 1$. Fig. 2 shows the ratio of the lower bound of the CFI of fin-SPADE to the QFI [24]. It clearly shows that for a large number of signal photons ηN_s , the ratio converges to the unity, which indicates that the fin-SPADE measurement is optimal in that regime. Even when ηN_s is small, the lower bound of the CFI gives at least 65% of the QFI. Hence, the fin-SPADE method's performance is not degraded significantly by thermal noise compared to the QFI. A particular way to improve this further is to directly measure the incoming photon numbers onto the symmetric and antisymmetric modes and their derivative modes $\{\hat{a}_\pm, \hat{b}_\pm\}$ [24]. In general, the implementation of such a measurement requires a prior information, which might be overcome by using adaptive method [45].

Conclusions and discussion.— In this Letter, we have investigated the effect of noise on the resolution of two identical sources with an arbitrary state using quantum and classical Fisher information and shown that the Fisher information converges to zero if the system suffers from false excitation noise such as thermal noise or dark counts. We have shown that in the problem of resolving two incoherent thermal sources with the number of signal photons being larger than that of noise photons, a signal-to-noise ratio poses a fundamental limit. Finally, we have shown that the finite spatial demultiplexing measurement is nearly optimal for a large signal-to-noise ratio.

Throughout the Letter, we are assuming that two objects are identical. Thus, the same conclusion might not hold if the sources are not identical [46–49]. It would

be interesting to analyze the problem of resolving non-identical sources.

We acknowledge useful discussions with Cosmo Lupo. We acknowledge support from the ARL-CDQI (W911NF-15-2-0067), ARO (W911NF-18-1-0020, W911NF-18-1-0212), ARO MURI (W911NF-16-1-0349), AFOSR MURI (FA9550-15-1-0015, FA9550-19-1-0399), DOE (DE-SC0019406), NSF (EFMA-1640959, OMA-1936118), and the Packard Foundation (2013-39273).

* changhun@uchicago.edu

† liang.jiang@uchicago.edu

- [1] L. Rayleigh, “XXXI. Investigations in optics, with special reference to the spectroscope,” *Philos. Mag. Ser. 5* **8**, 261–274 (1879).
- [2] M. Born and E. Wolf, *Principles of optics: electromagnetic theory of propagation, interference and diffraction of light* (Elsevier, 2013).
- [3] M. Tsang, R. Nair, and X.-M. Lu, “Quantum theory of superresolution for two incoherent optical point sources,” *Phys. Rev. X* **6**, 031033 (2016).
- [4] R. Nair and M. Tsang, “Far-field superresolution of thermal electromagnetic sources at the quantum limit,” *Phys. Rev. Lett.* **117**, 190801 (2016).
- [5] C. Lupo and S. Pirandola, “Ultimate precision bound of quantum and subwavelength imaging,” *Phys. Rev. Lett.* **117**, 190802 (2016).
- [6] S. Z. Ang, R. Nair, and M. Tsang, “Quantum limit for two-dimensional resolution of two incoherent optical point sources,” *Phys. Rev. A* **95**, 063847 (2017).
- [7] Z. Yu and S. Prasad, “Quantum limited superresolution of an incoherent source pair in three dimensions,” *Phys. Rev. Lett.* **121**, 180504 (2018).
- [8] C. Napoli, S. Piano, R. Leach, G. Adesso, and T. Tufarelli, “Towards superresolution surface metrology: Quantum estimation of angular and axial separations,” *Phys. Rev. Lett.* **122**, 140505 (2019).
- [9] J. S. Sidhu and P. Kok, “Quantum metrology of spatial deformation using arrays of classical and quantum light emitters,” *Phys. Rev. A* **95**, 063829 (2017).
- [10] M. Tsang, “Subdiffraction incoherent optical imaging via spatial-mode demultiplexing,” *New J. Phys.* **19**, 023054 (2017).
- [11] S. Zhou and L. Jiang, “Modern description of rayleigh’s criterion,” *Phys. Rev. A* **99**, 013808 (2019).
- [12] M. Tsang, “Quantum limit to subdiffraction incoherent optical imaging,” *Phys. Rev. A* **99**, 012305 (2019).
- [13] C. Lupo, Z. Huang, and P. Kok, “Quantum limits to incoherent imaging are achieved by linear interferometry,” *Phys. Rev. Lett.* **124**, 080503 (2020).
- [14] X.-M. Lu, H. Krovi, R. Nair, S. Guha, and J. H. Shapiro, “Quantum-optimal detection of one-versus-two incoherent optical sources with arbitrary separation,” *npj Quantum Inf.* **4**, 1–8 (2018).
- [15] S. Pirandola, R. Laurenza, C. Lupo, and J. L. Pereira, “Fundamental limits to quantum channel discrimination,” *npj Quantum Inf.* **5**, 1–8 (2019).
- [16] M. Paúr, B. Stoklasa, Z. Hradil, L. L. Sánchez-Soto, and J. Rehacek, “Achieving the ultimate optical resolution,”

- Optica **3**, 1144–1147 (2016).
- [17] Z. S. Tang, K. Durak, and A. Ling, “Fault-tolerant and finite-error localization for point emitters within the diffraction limit,” *Optics express* **24**, 22004–22012 (2016).
- [18] F. Yang, A. Tashchilina, E. S. Moiseev, C. Simon, and A. I. Lvovsky, “Far-field linear optical superresolution via heterodyne detection in a higher-order local oscillator mode,” *Optica* **3**, 1148–1152 (2016).
- [19] W.-K. Tham, H. Ferretti, and A. M. Steinberg, “Beating rayleigh’s curse by imaging using phase information,” *Phys. Rev. Lett.* **118**, 070801 (2017).
- [20] M. Parniak, S. Borówka, K. Boroszko, W. Wasilewski, K. Banaszek, and R. Demkowicz-Dobrzański, “Beating the rayleigh limit using two-photon interference,” *Phys. Rev. Lett.* **121**, 250503 (2018).
- [21] Y. L. Len, C. Datta, M. Parniak, and K. Banaszek, “Resolution limits of spatial mode demultiplexing with noisy detection,” *Int. J. Quantum Inf* **18**, 1941015 (2020).
- [22] M. Gessner, C. Fabre, and N. Treps, “Superresolution limits from measurement crosstalk,” *Phys. Rev. Lett.* **125**, 100501 (2020).
- [23] C. Lupo, “Subwavelength quantum imaging with noisy detectors,” *Phys. Rev. A* **101**, 022323 (2020).
- [24] “Supplementary material,”.
- [25] C. W. Helstrom and C. W. Helstrom, *Quantum detection and estimation theory*, Vol. 3 (Academic press New York, 1976).
- [26] A. S. Holevo, *Probabilistic and statistical aspects of quantum theory*, Vol. 1 (Springer Science & Business Media, 2011).
- [27] S. L. Braunstein and C. M. Caves, “Statistical distance and the geometry of quantum states,” *Phys. Rev. Lett.* **72**, 3439 (1994).
- [28] M. G. A. Paris, “Quantum estimation for quantum technology,” *Int. J. Quantum Inf* **7**, 125–137 (2009).
- [29] D. F. Walls and G. J. Milburn, *Quantum optics* (Springer Science & Business Media, 2007).
- [30] We assume that the series always converge to focus on physically relevant situations.
- [31] T. Gefen, A. Rotem, and A. Retzker, “Overcoming resolution limits with quantum sensing,” *Nat. commun.* **10**, 4992 (2019).
- [32] O. Pinel, P. Jian, N. Treps, C. Fabre, and D. Braun, “Quantum parameter estimation using general single-mode Gaussian states,” *Phys. Rev. A* **88**, 040102 (2013).
- [33] Z. Jiang, “Quantum Fisher information for states in exponential form,” *Phys. Rev. A* **89**, 032128 (2014).
- [34] D. Šafránek, A. R. Lee, and I. Fuentes, “Quantum parameter estimation using multi-mode Gaussian states,” *New J. Phys.* **17**, 073016 (2015).
- [35] D. Šafránek and I. Fuentes, “Optimal probe states for the estimation of Gaussian unitary channels,” *Phys. Rev. A* **94**, 062313 (2016).
- [36] R. Nichols, P. Liuzzo-Scorpo, P. A. Knott, and G. Adesso, “Multiparameter Gaussian quantum metrology,” *Phys. Rev. A* **98**, 012114 (2018).
- [37] D. Šafránek, “Estimation of Gaussian quantum states,” *J. Phys. A Math. Theor.* **52**, 035304 (2018).
- [38] C. Oh, C. Lee, L. Banchi, S.-Y. Lee, C. Rockstuhl, and H. Jeong, “Optimal measurements for quantum fidelity between Gaussian states and its relevance to quantum metrology,” *Phys. Rev. A* **100**, 012323 (2019).
- [39] C. R. Rao, “Information and the accuracy attainable in the estimation of statistical parameters,” in *Breakthroughs in statistics* (Springer, 1992) pp. 235–247.
- [40] S. M. Kay, *Fundamentals of statistical signal processing* (Prentice Hall PTR, 1993).
- [41] H. Cramér, *Mathematical methods of statistics*, Vol. 43 (Princeton university press, 1999).
- [42] H. L. Van Trees, *Detection, estimation, and modulation theory, part I: detection, estimation, and linear modulation theory* (John Wiley & Sons, 2004).
- [43] F. Yang, R. Nair, M. Tsang, C. Simon, and A. I. Lvovsky, “Fisher information for far-field linear optical superresolution via homodyne or heterodyne detection in a higher-order local oscillator mode,” *Phys. Rev. A* **96**, 063829 (2017).
- [44] M. Stein, A. Mezghani, and J. A. Nossek, “A lower bound for the Fisher information measure,” *IEEE Signal Process. Lett.* **21**, 796–799 (2014).
- [45] O. E. Barndorff-Nielsen and R. D. Gill, “Fisher information in quantum statistics,” *J. Phys. A Math. Theor.* **33**, 4481 (2000).
- [46] J. Řeháček, Z. Hradil, B. Stoklasa, M. Paúr, J. Grover, A. Krzic, and L. L. Sánchez-Soto, “Multiparameter quantum metrology of incoherent point sources: towards realistic superresolution,” *Phys. Rev. A* **96**, 062107 (2017).
- [47] J. Řeháček, Z. Hradil, D. Koutný, J. Grover, A. Krzic, and L. L. Sánchez-Soto, “Optimal measurements for quantum spatial superresolution,” *Phys. Rev. A* **98**, 012103 (2018).
- [48] K. A. G. Bonsma-Fisher, W.-K. Tham, H. Ferretti, and A. M. Steinberg, “Realistic sub-rayleigh imaging with phase-sensitive measurements,” *New J. Phys.* **21**, 093010 (2019).
- [49] S. Prasad, “Quantum limited super-resolution of an unequal-brightness source pair in three dimensions,” *Phys. Scr.* **95**, 054004 (2020).